

# The chemistry of novolac resins: 3. $^{13}\text{C}$ and $^{15}\text{N}$ n.m.r. studies of curing with hexamethylenetetramine

Xiaoqing Zhang, Mark G. Looney and David H. Solomon\*

Department of Chemical Engineering, The University of Melbourne, Parkville,  
VIC 3052, Australia

and Andrew K. Whittaker

Centre of Magnetic Resonance, The University of Queensland, Brisbane,  
QLD 4072, Australia

(Received 25 November 1996; revised 6 February 1997)

The reactions between novolac resins and hexamethylenetetramine (HMTA) which occur on curing have been studied by  $^{13}\text{C}$  and  $^{15}\text{N}$  high-resolution n.m.r. in both solution and the solid state. Strong evidence for the existence of many curing intermediates is obtained. New curing intermediates are reported along with experimental data to support previously postulated intermediates. The initial curing reactions between novolac and HMTA produce various substituted benzoxazines and benzylamines. Thermal decomposition/oxidation and further reactions of these initial intermediates generate methylene linkages between phenolic rings for chain extension and cross-linking. Among the three kinds of methylene linkages, the *para-para* methylene linkages are formed at relatively lower temperatures. Various imine, amide and imide side-products also concurrently appear during the process. The initial amount of HMTA plays a critical role in the curing reactivity and chemical structures of the cured resins. The lower the amount of HMTA, the lower the temperature at which curing occurs, and the lower the amount of the nitrogen-containing side-products in the finally cured resins. The *ortho*-linked intermediates are relatively stable, and can remain in the cured resins up to higher temperatures. The study provides an extensive description of the curing reactions of novolac resins. © 1997 Elsevier Science Ltd.

(Keywords: novolac resins; curing chemistry; cross-linked polymers)

## INTRODUCTION

Phenol-formaldehyde resins were the first totally synthetic commercial polymer resins, and were first described over 100 years ago. Because of their low cost, dimensional stability, age resistance and high tensile strength, the resins have been used commercially in many applications such as moulding compounds, laminates, adhesives and shell moulds for metals and electrical insulation. Over the past 50 years, a great deal of effort has been expended towards the understanding of the curing chemistry of these resins<sup>1–4</sup>. Most available chemical and physical analytical techniques have been applied. However, because the curing reactions are very complicated and the cured resins are inevitably highly cross-linked materials which do not melt or dissolve, most techniques are difficult to use or fail to provide significant structural information. A detailed knowledge of the curing chemistry, which is responsible for many desired properties, and fundamental to extending the application and modification of the resins, has yet not been achieved.

Solid state high-resolution n.m.r. techniques make it possible to carry out direct structural studies on cured commercial phenolic resins<sup>5–13</sup>. These studies, combined

with the results on various small molecular model systems by solution n.m.r.<sup>14–20</sup>, have given a large amount of information about the curing intermediates and allowed speculation on curing mechanisms. Among the reports on phenolic resins,  $^{13}\text{C}$ -labelled formaldehyde<sup>5</sup> and  $^{13}\text{C}$ -labelled or  $^{15}\text{N}$ -labelled hexamethylenetetramine (HMTA)<sup>10</sup> have been used to study the curing reactions. The chemical shift changes of these enriched resonances in  $^{13}\text{C}$  or  $^{15}\text{N}$  CP/MAS spectra throughout the curing process gave information on the chemical structures of the cured resins. This was demonstrated in Hatfield and Maciel's work<sup>10</sup>, in which 15 possible intermediates were considered. The nature of these chemical structures in terms of chemical shifts was examined under various conditions. They confirmed that the curing resulted in increased methylene cross-linking, and these methylene bridges originated from HMTA. In addition, they also drew a comparison between their results and those of solution NMR. Their work constitutes a primary element of our current study of the curing chemistry of phenolic resins. However, there still remain many aspects which require further clarification.

In this paper,  $^{13}\text{C}$  and  $^{15}\text{N}$  high-resolution n.m.r. spectra in both solution and the solid state were measured for cured resins to follow the curing process.

\* To whom correspondence should be addressed

The curing reagent HMTA was labelled with both  $^{13}\text{C}$  and  $^{15}\text{N}$  to enhance the signals. We not only varied the amount of the curing reagent over a wide range, but also performed the curing process under carefully controlled conditions to allow maximum opportunities to observe intermediates formed during the curing. We give a comprehensive description of the structures of intermediates in the curing of novolac resins with HMTA, including those which were postulated as intermediates previously but for which experimental evidence was lacking. The reaction mechanisms are discussed in detail.

## EXPERIMENTAL

### Samples

The conventional novolac resins used in this study contain 0.15% free phenol, and the number-averaged chain-length is about eight phenolic repeat units, comprising 25% *ortho-ortho*, 53% *ortho-para* and 22% *para-para* methylene linkages as determined by the  $^{13}\text{C}$  solution n.m.r. spectrum. The *ortho*- and *para*-unsubstituted phenolic positions of the resins can be considered as reactive sites, and the ratio of *ortho:para* sites of the resin is 88:12. The  $^{13}\text{C}$ - and  $^{15}\text{N}$ -labelled HMTA was synthesized using 99%  $^{13}\text{C}$ -enriched formaldehyde and 99%  $^{15}\text{N}$ -enriched ammonia.

The HMTA content of novolac/HMTA (N/H) samples was varied in weight ratios of 80/20, 88/12 and 94/6. Novolac and HMTA were mixed in a methanol/acetone (6/4) solvent (5% w/v) at room temperature. After removing the solvent and drying the mixture at 50°C *in vacuo*, the samples were cured in a Eurotherm 902 oven. The samples were heated to 90°C for 6 h, then the curing temperature was increased at a rate of 3.7°C h<sup>-1</sup> until 135°C, thereafter at 12°C h<sup>-1</sup> until 205°C, and finally kept at 205°C for 4 h. In order to study the structural change of the novolac resins during the curing process, samples were taken from the oven after being cured to 90°C for 6 h, at 105, 120, 135, 160, 185 and 205°C, and finally after heating at 205°C for 4 h.

### N.m.r. experiments

Solution  $^{13}\text{C}$  n.m.r. spectra were recorded immediately after dissolving the samples in acetone-*d*<sub>6</sub> (99.9%) solvent on using a JEOL JNM-GX400 n.m.r. spectrometer at resonance frequencies of 100 MHz for carbon-13. Solid state n.m.r. experiments were carried out using a Bruker MSL200 spectrometer at resonance frequencies of 200 MHz for proton, 50.4 MHz for carbon-13 and 20.3 MHz for nitrogen-15, respectively. High-resolution  $^{13}\text{C}$  and  $^{15}\text{N}$  n.m.r. in the solid state was performed using CP, MAS and high-power dipolar decoupling (DD) techniques.  $^{13}\text{C}$  CP/MAS spectra were observed at a contact time of CP of 1.5 ms and a repetition time of 2 s.  $^{13}\text{C}$  dipolar dephased spectra were observed after a 75 μs decoupling delay after CP. For  $^{15}\text{N}$  CP/MAS spectra, the contact time was 2 ms while the repetition time was 2 s. The decoupling delay time was set at 100 or 135 μs for observation of  $^{15}\text{N}$  dipolar dephased spectra. The rate of MAS was 4.1–5.1 kHz. The chemical shift of  $^{13}\text{C}$  spectra was determined by taking the methine carbon of solid adamantane (29.5 ppm relative to tetramethylsilane) as an external reference standard. For  $^{15}\text{N}$  spectra, the  $^{15}\text{N}$  resonance of 99% labelled

HMTA at 44.0 ppm (relative to liquid NH<sub>3</sub> at 25°C) was taken as an external reference.

## RESULTS AND DISCUSSION

Various intermediates suggested as being involved in the curing of novolacs with HMTA, or of interest in our study, are summarized in *Table 1*. The  $^{13}\text{C}$  and  $^{15}\text{N}$  chemical shifts of these structures are taken from previous reports, values of similar structures and from our studies of model compounds (see references cited in the table). The numbers of the structures in the text are referenced to those in *Table 1*.

### $^{13}\text{C}$ n.m.r. spectra of cured novolac resins

The curing reactions between novolac resins and HMTA started at 90–120°C, and the sample remained soluble in a solvent, such as acetone. Thus, it was possible to study the initial reactions by solution n.m.r. techniques.  $^{13}\text{C}$  solution n.m.r. spectra of the novolac before curing (in methanol-*d*<sub>4</sub>) and the N/H = 80/20 samples after curing to 90, 105 and 120°C (in acetone-*d*<sub>6</sub>) are shown in *Figure 1*. The resonances of the novolac at 116 and 121 ppm are due to *ortho*- and *para*-unsubstituted phenolic carbons, while those at 150–156 and 127–135 ppm are due to hydroxyl-substituted carbons and the other phenolic carbons, respectively. The *para-para*, *para-ortho* and *ortho-ortho* methylene linkages in the resins appear at 40.8, 35.5 and 31.5 ppm, respectively. The strong resonance at 74.5 ppm in the N/H = 80/20 samples corresponds to HMTA resonances.

Curing N/H = 80/20 to 90°C for 6 h generated various minor resonances at 68–86 ppm. Among these, the narrow peaks at 85.9 and 81.4 ppm correspond to the methylene carbons in HOCH<sub>2</sub>OCH<sub>2</sub>OH and HOCH<sub>2</sub>OH<sup>14</sup> which originate from the hydration/oxidation of molecular pieces broken down from HMTA<sup>4</sup>. The resonances at 71.1 and 68.2 ppm are consistent with *para*- and *ortho*-linked dimethylene ether structures as shown in *Table 1* (4), where the 71.1 ppm peak appeared first. Various substituted benzoxazines (5) and benzylamines (6)–(8) (at 78–84 and 39–57 ppm) could be observed when the curing temperature reached 105°C. Curing up to 120°C caused a certain extent of cross-linking, and approximately 50% of the cured sample could be dissolved. The n.m.r. spectrum of the soluble part showed various significant resonances over a wide chemical shift range (192, 170–160 and 85–35 ppm). Note that the major structures present at that time were various substituted benzoxazines (78–84, 55, 49–50 and 41 ppm), benzylamines (44–46 ppm), and di- and tribenzylamines (50, 52, 57 ppm) ((5)–(8)), together with a minor amount of diamine- and triazine-type structures (e.g. (9), (10)). The 192 ppm peak is due to the *para*-hydroxybenzaldehyde –CHO carbons (15)-2. The resonances at 161–168 ppm suggest that amides (11), imides (12) and/or imines (13) were also present. At this stage the quantity of these intermediates was very small since the curing reactions had just started. The readily observed resonances of these intermediates indicate that they originate from the –CH<sub>2</sub>– of HMTA (99%  $^{13}\text{C}$  enriched). Further curing above 135°C gave more insoluble products, and only some small molecular species (such as HOCH<sub>2</sub>OCH<sub>2</sub>OH and HOCH<sub>2</sub>OH) remained in the solution.

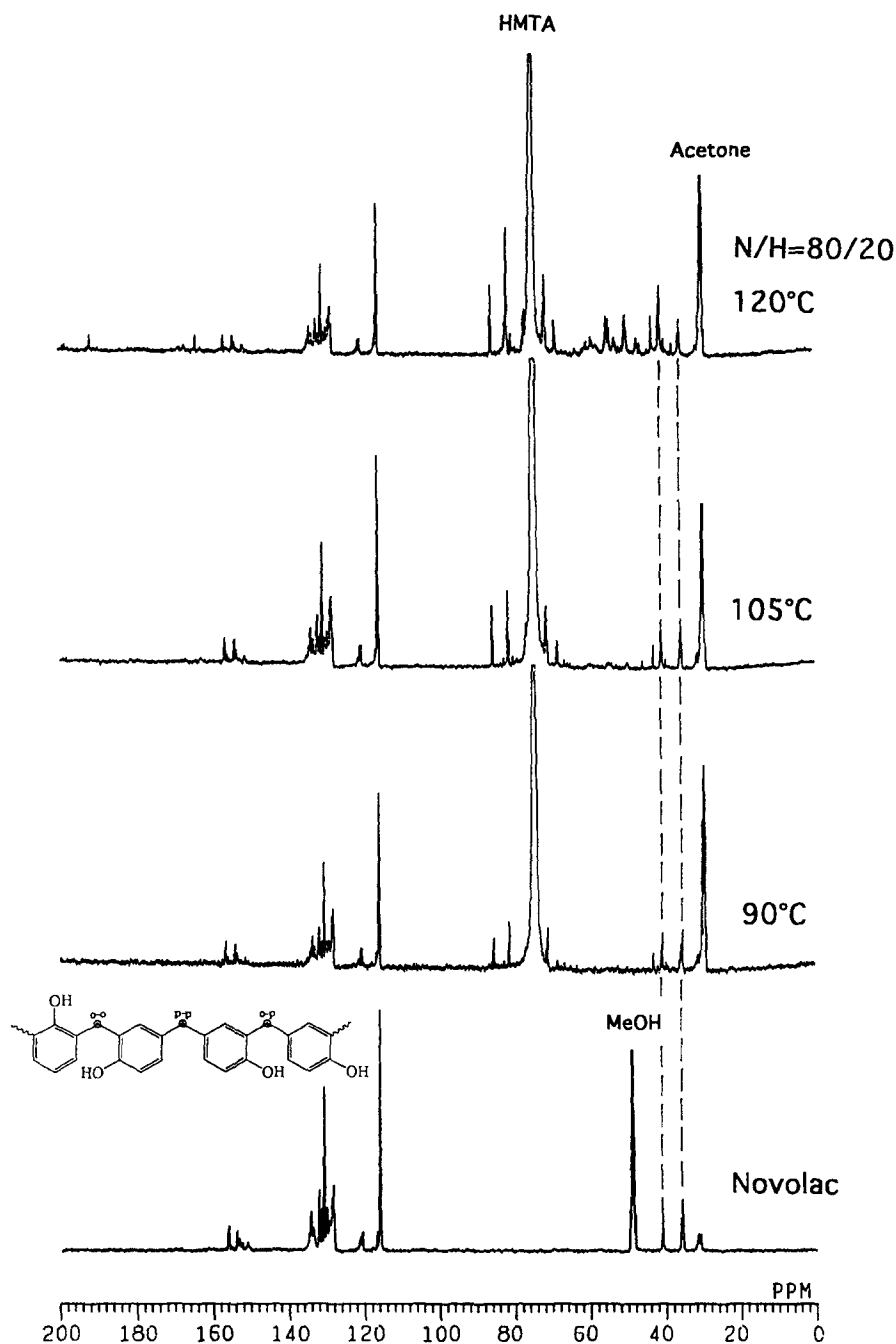


**Figure 1**  $^{13}\text{C}$  solution n.m.r. spectra of novolac before curing (in MeOD) and novolac/HMTA = 80/20 samples cured to 90°C/6 h, 105°C and 120°C

$^{13}\text{C}$  CP/MAS n.m.r. spectra of the N/H = 80/20 samples after curing are shown in *Figure 2*. At 90°C, the strong peak of HMTA (99%  $^{13}\text{C}$  enriched) is dominant, while the natural-abundance signals of novolac resins are very weak. All strong resonances observed at higher temperatures can be assigned to the curing intermediates derived from HMTA.  $^{13}\text{C}$  resonances at 53 ppm (40–60 ppm) and 82 ppm (diagnostic for benzoxazines, which is broader than the resonance in HO-CH<sub>2</sub>-OH, appeared as a left shoulder to the strong HMTA peak) were observed at 120°C, and are consistent with the initial curing intermediates, i.e. various substituted benzoxazines and benzylamines, as found in the  $^{13}\text{C}$  solution spectra. Increasing the curing temperature decreased the intensity of the HMTA while the resonances at 82 and 53 ppm increased. The resonances around 53 ppm (40–60 ppm) became

dominant at 160°C due to the formation of a large amount of benzoxazine and benzylamine intermediates (5)–(8). Above 185°C, the HMTA resonance was very weak, while the peak at 82 ppm also began to decrease in intensity with a further increase in the curing temperature. After curing to 135°C, a shoulder at 35 ppm appeared due to the formation of *ortho-ortho*, *ortho-para* and *para-para* methylene linkages, which appeared as a single peak because of linewidth overlapping. Note that the 35 ppm peak increased in intensity with increased curing temperatures, and became strong after curing samples to 205°C/4 h. At higher temperatures, resonances at 16 and 195 ppm also became pronounced, corresponding to the formation of methyl and aldehyde substituents mainly at the *ortho*-phenolic positions (15)-1 and (15)-2, because the *ortho*-reactive sites are dominant in the resins

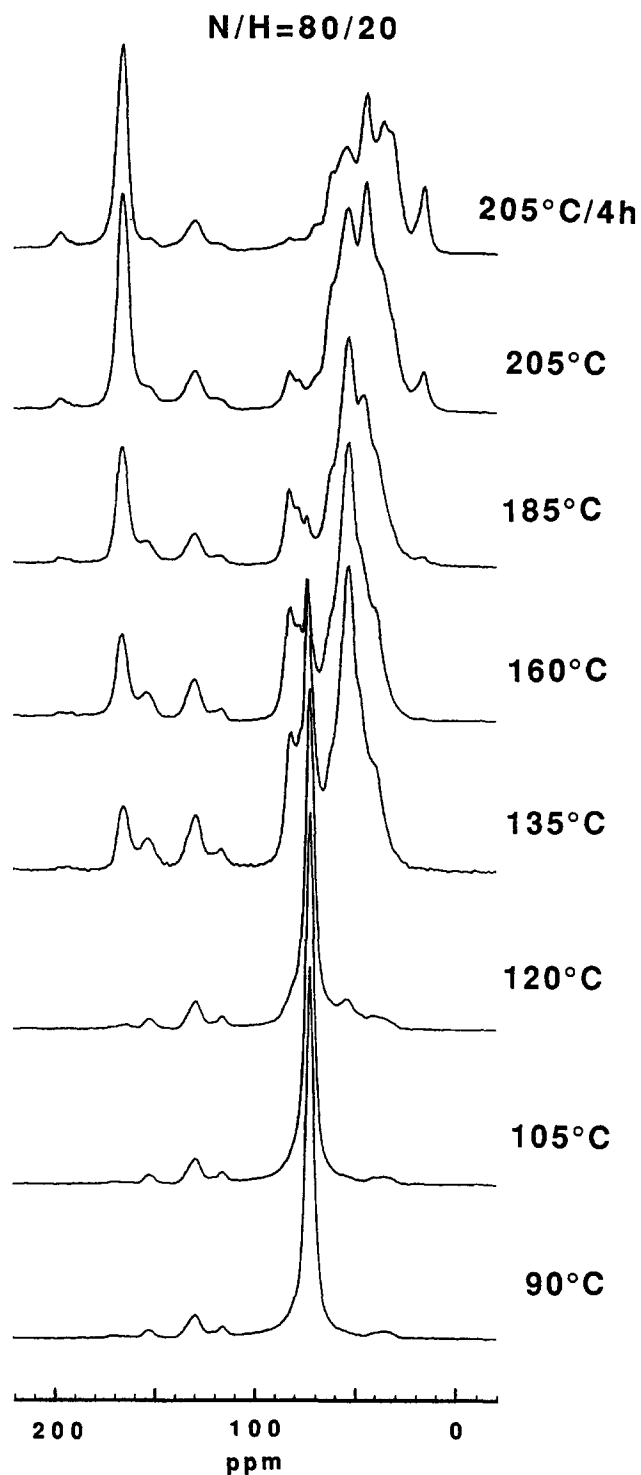


Figure 2  $^{13}\text{C}$  CP/MAS n.m.r. spectra of novolac/HMTA = 80/20 samples after curing (MAS rate = 5.0–5.1 kHz)

before curing. The signal at 165 ppm became apparent at 135°C, and remained throughout the curing process. The dipolar dephase experiment should provide additional information about this signal.

Only non-protonated and mobile resonances can be observed in  $^{13}\text{C}$  CP/MAS dipolar dephased spectra. As expected, the peaks due to substituted phenolic carbons at 152 and 130 ppm are still present after a 75  $\mu\text{s}$  decoupling delay after CP (Figure 3). The mobile HMTA molecules were also detected in the samples cured below 185°C, but they disappeared at higher temperatures. Note that the carbon resonances around 165 ppm in imines (Table 1, (13)) all have one hydrogen

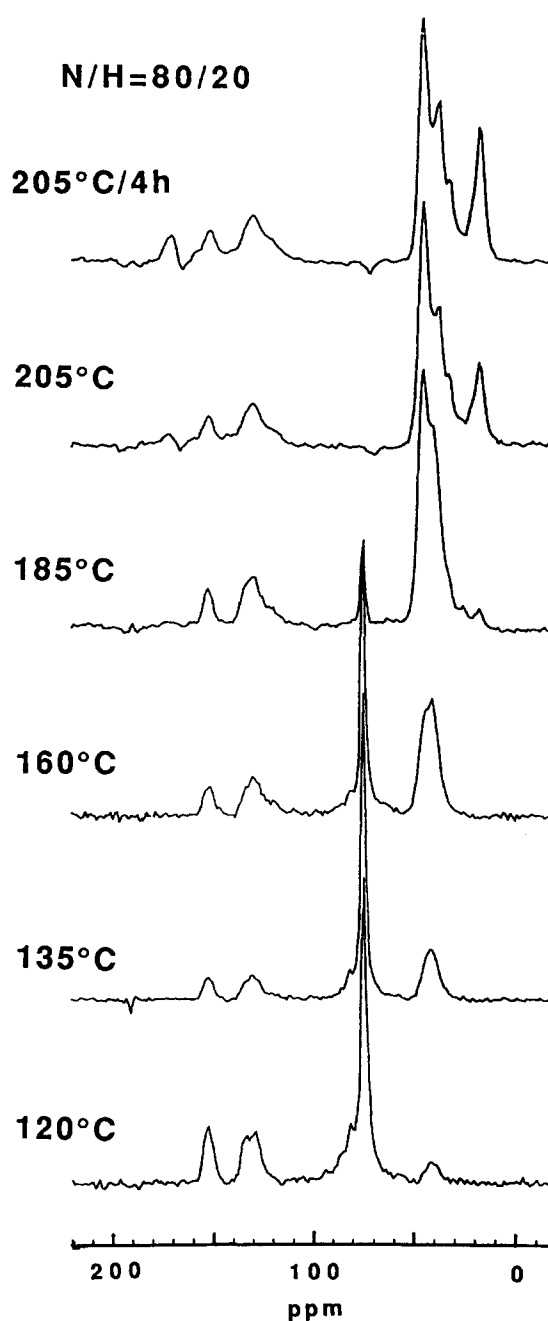
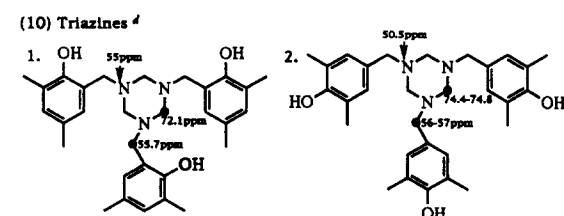
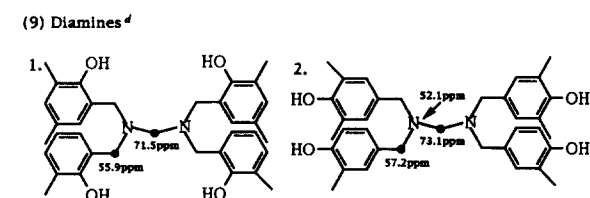
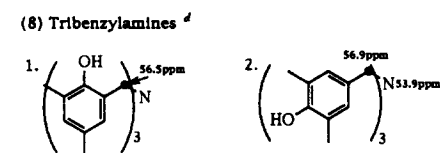
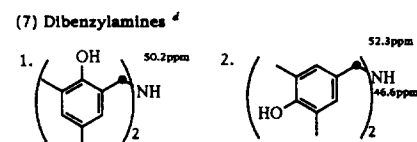
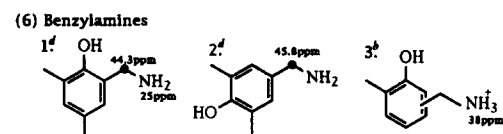
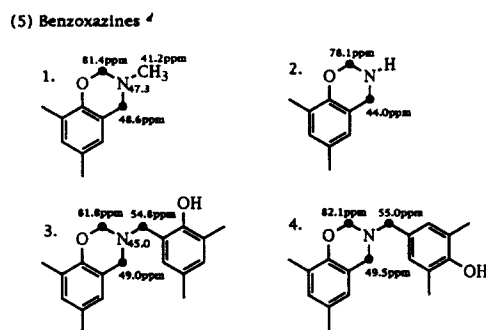
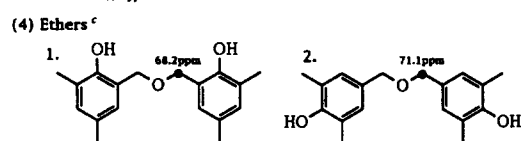
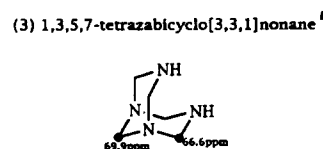
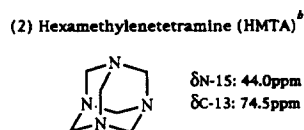
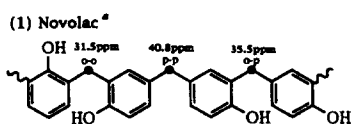


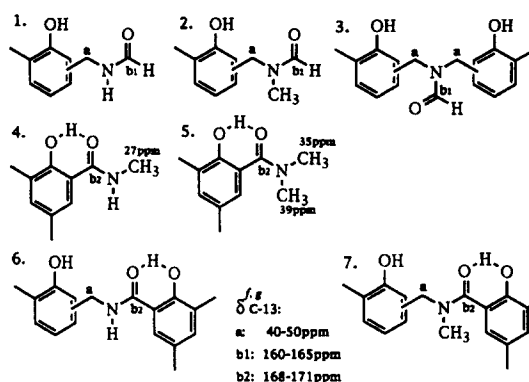
Figure 3  $^{13}\text{C}$  CP/MAS n.m.r. dipolar dephased spectra (75  $\mu\text{s}$  decoupling delay) of novolac/HMTA = 80/20 samples after curing (MAS rate = 5.0–5.1 kHz)

atom attached. Some carbonyl carbons of amides/imides (b1 in (11) and (12)) also have one bonded hydrogen. For the samples cured below 205°C, the peak at 165 ppm disappeared after a 75  $\mu\text{s}$  decoupling delay. Above 205°C, the peak could still be detected, but it shifts to 169 ppm. This indicates that the carbonyl carbons without attached hydrogens in amides/imides (b2 in (11) and (12)) only appear at 205°C, and their resonances are located 4 ppm downfield. The  $^{15}\text{N}$  chemical shifts of amides, imides and imines are quite different.  $^{15}\text{N}$  CP/MAS spectra can provide further details, as discussed later in this paper. Dipolar dephased spectra confirm that the peak at 16 ppm is due to the methyl groups on phenolic rings, since mobile methyl carbons should still remain in the dipolar dephasing experiment. The strong resonances at 35–45 ppm after the decoupling delay suggest the existence of other kinds of mobile

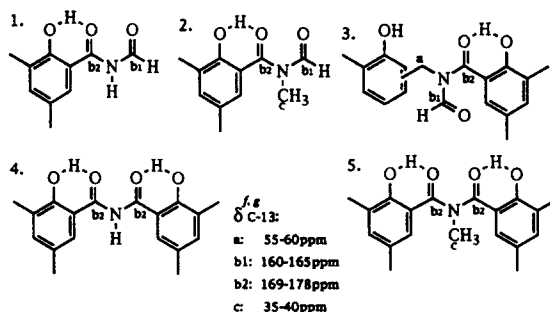
Table 1 Structures and key n.m.r. data of possible curing intermediates



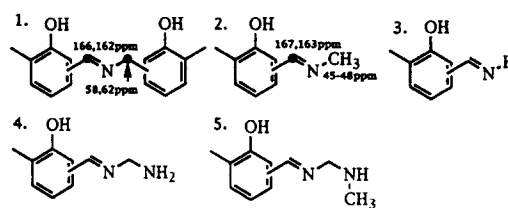
(11) Amides (δ<sup>f</sup> N-15: 110-130ppm)



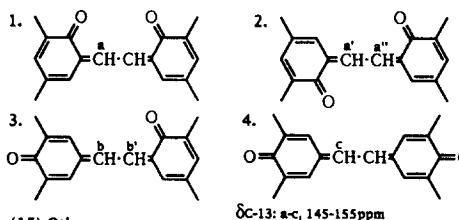
(12) Imides (δ<sup>f</sup> N-15: 145-155ppm)



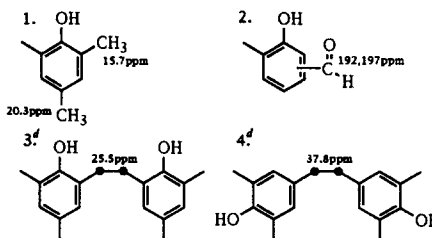
(13) Imines<sup>d,f</sup> (δ<sup>f</sup> N-15 290-350ppm)



(14) Stilbenequinones<sup>h</sup>



(15) Others



<sup>a</sup> This work, described in the text  
<sup>b</sup> Values taken from Hatfield and Maciel<sup>10</sup>  
<sup>c</sup> Values taken from Chuang and Maciel<sup>13</sup>  
<sup>d</sup> Values taken from Potter<sup>21</sup>  
<sup>e</sup> Values taken from similar structures in Levy and Lichter<sup>22</sup>  
<sup>f</sup> Values taken from similar structures in Sadtler Research Laboratories<sup>23</sup>  
<sup>g</sup> Values taken from similar structures in Levy *et al.*<sup>24</sup>  
<sup>h</sup> From Mihajlovic and Cekovic<sup>25</sup>

methyl groups in structures of amides/imides and imines such as (11)-2, -4, -5 and 7, (12)-2 and -5, and (13)-2 shown in Table 1.

Decreasing the amount of HMTA was found to change the curing process.  $^{13}\text{C}$  solution n.m.r. spectra of N/H = 88/12 and 94/6 samples after curing to 90, 105 and 120°C are shown in Figures 4 and 5. Compared to those of the cured N/H = 80/20 samples, the lower initial HMTA content appears to lower the temperature at which the curing begins. The  $^{13}\text{C}$  spectrum of the N/H = 88/12 sample cured to 90°C is quite similar to that of the N/H = 80/20 samples at 105°C. Furthermore, for the 94/6 system the spectrum of the sample cured to 90°C is comparable to those of the 80/20 sample at 120°C and the 88/12 sample at 105°C. When the N/H = 94/6 sample was cured to 105 and 120°C, we

could even observe signals of methyl groups which were found for the 80/20 sample after curing to 185°C. In the spectrum of the N/H = 94/6 sample, signals at 85.9 and 81.4 ppm and the ether intensities decreased with increasing curing temperature and their resonances disappeared above 120°C, while the HMTA signal at 74.5 ppm was still present. Then, the main intermediates were substituted benzylamines (6)–(8) with  $^{13}\text{C}$  chemical shifts in the range 45–60 ppm. The benzoxazine intermediates were not observed in the system. Note that the peak due to *para-para* methylene linkages at 40.8 ppm significantly increased upon curing the N/H = 94/6 sample to 120°C, together with the resonance at 37.8 ppm due to *para-para* -CH<sub>2</sub>-CH<sub>2</sub>-ethylene linkages as shown in Table 1, (15)-4.

Two new peaks at 152 and 148 ppm were observed in the

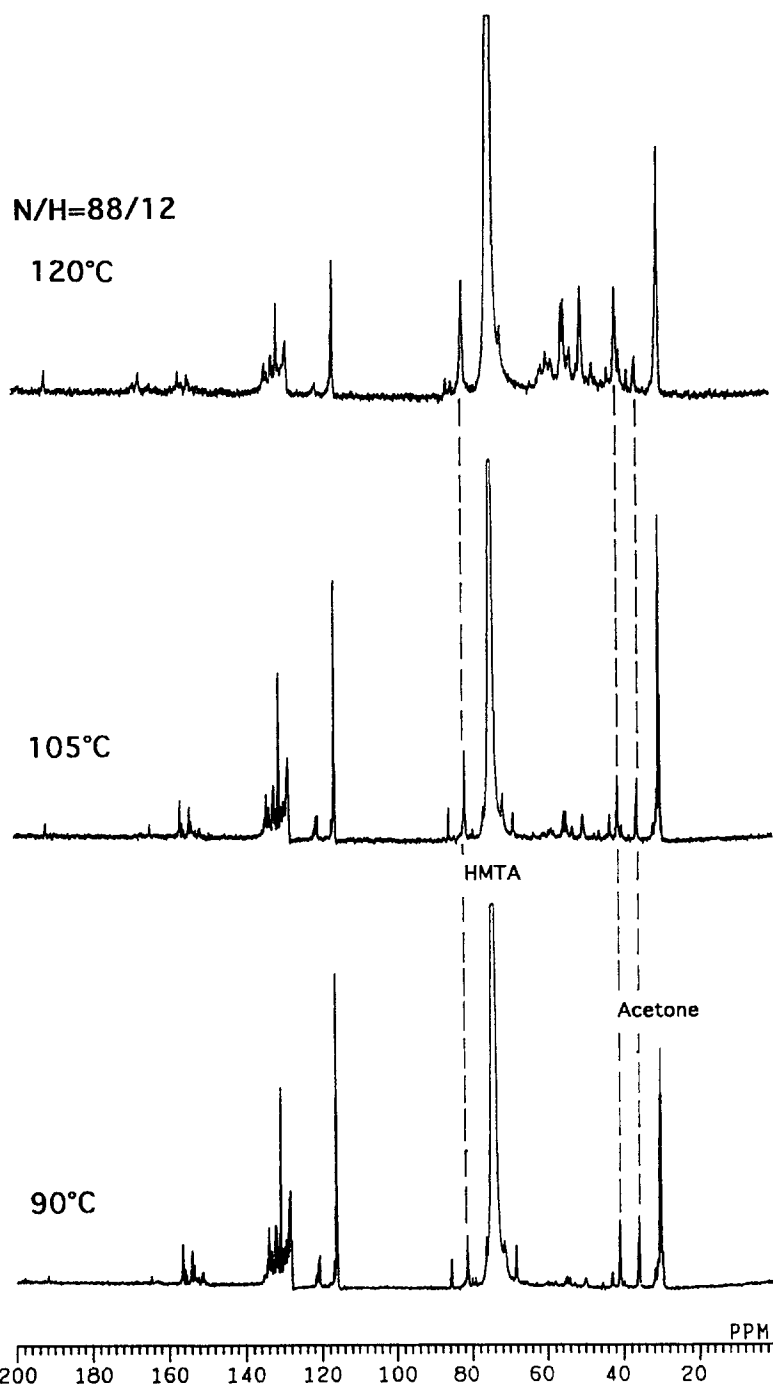


Figure 4  $^{13}\text{C}$  solution n.m.r. spectra of novolac/HMTA = 88/12 samples cured to 90°C/6h, 105°C and 120°C

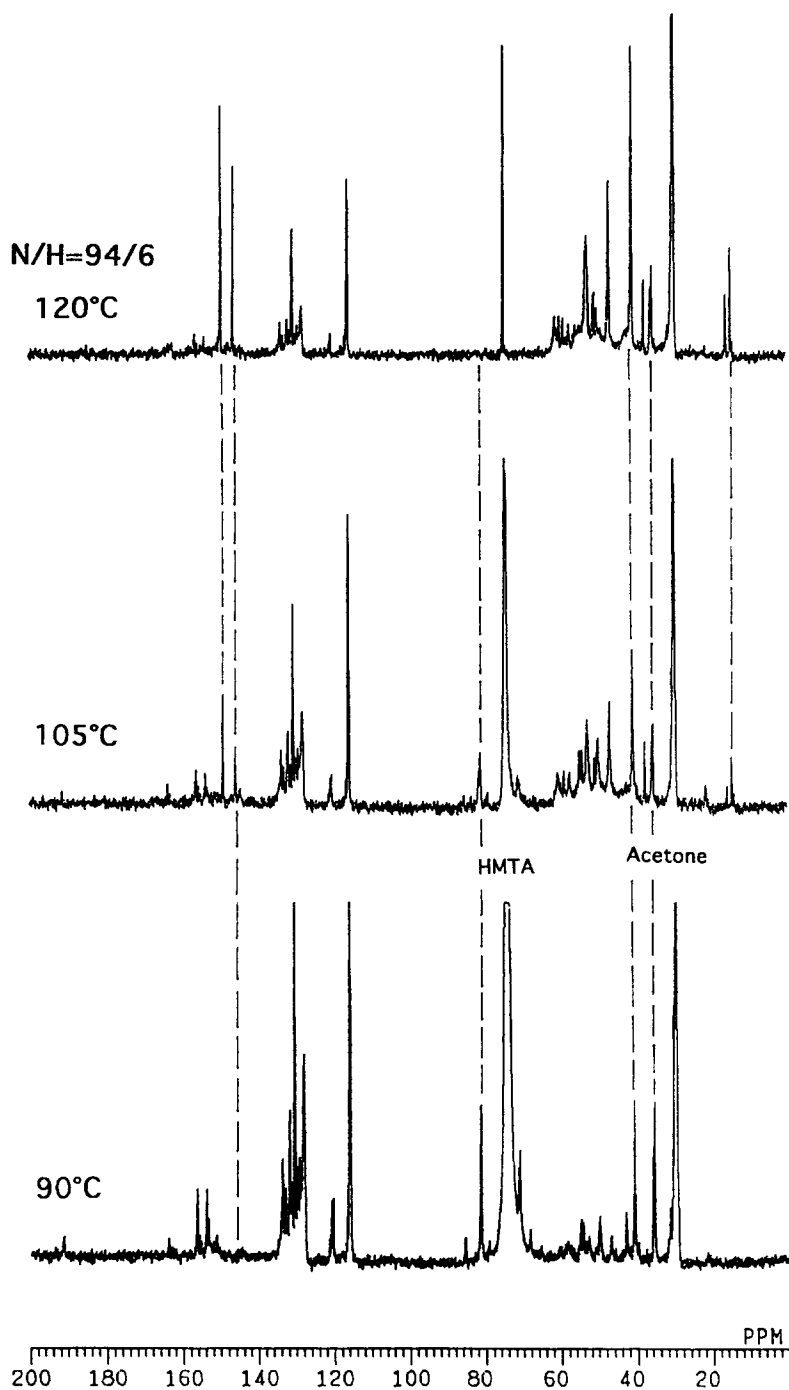


Figure 5  $^{13}\text{C}$  solution n.m.r. spectra of novolac/HMTA = 94/6 samples cured to 90°C/6 h, 105 and 120°C

spectrum of the 94/6 sample cured to 150°C, which were not found in the 80/20 and 88/12 systems. The intensities of the two peaks increased with increasing temperature. Since the two resonances are very strong (e.g. at 120°C in Figure 5), they must originate from the  $-\text{CH}_2-$  in HMTA.  $^{13}\text{C}$  DEPT spectra (distortionless enhancement by polarization transfer) indicate the two resonances are CH carbons; thus, they may be due to the methine carbons in stilbenequinone-type structures as shown in Table 1, (14).

$^{13}\text{C}$  CP/MAS spectra of cured N/H = 88/12 and 94/6 samples are shown in Figure 6. Several differences were observed for these systems compared with the N/H = 80/20 system, and these are outlined below:

(i) The HMTA signal disappears at lower temperatures when the initial amount of HMTA is lower. The HMTA

resonance in the 80/20 sample could be detected even at a curing temperature as high as 185°C, but disappeared at 160°C for the 88/12 system, and 135°C for the 94/6 system.

(ii) When the initial amount of HMTA is lower, the initial curing intermediates appear at lower temperatures, and then decompose at lower temperatures. The broad resonance at 82 ppm is indicative of benzoxazine structures (the carbon signal of  $\text{HO}-\text{CH}_2-\text{OH}$  is narrower and disappears above 120°C). As seen in  $^{13}\text{C}$  solution spectra, this resonance appeared as a left shoulder to that of HMTA in the CP/MAS spectra at 120°C, and 105°C for the 80/20 and 88/12 systems, but at 90°C for the 94/6 system (Figures 2 and 6). In the 80/20 and 88/12 systems, the intensity was the highest for the samples cured to 160°C, and remained in the finally

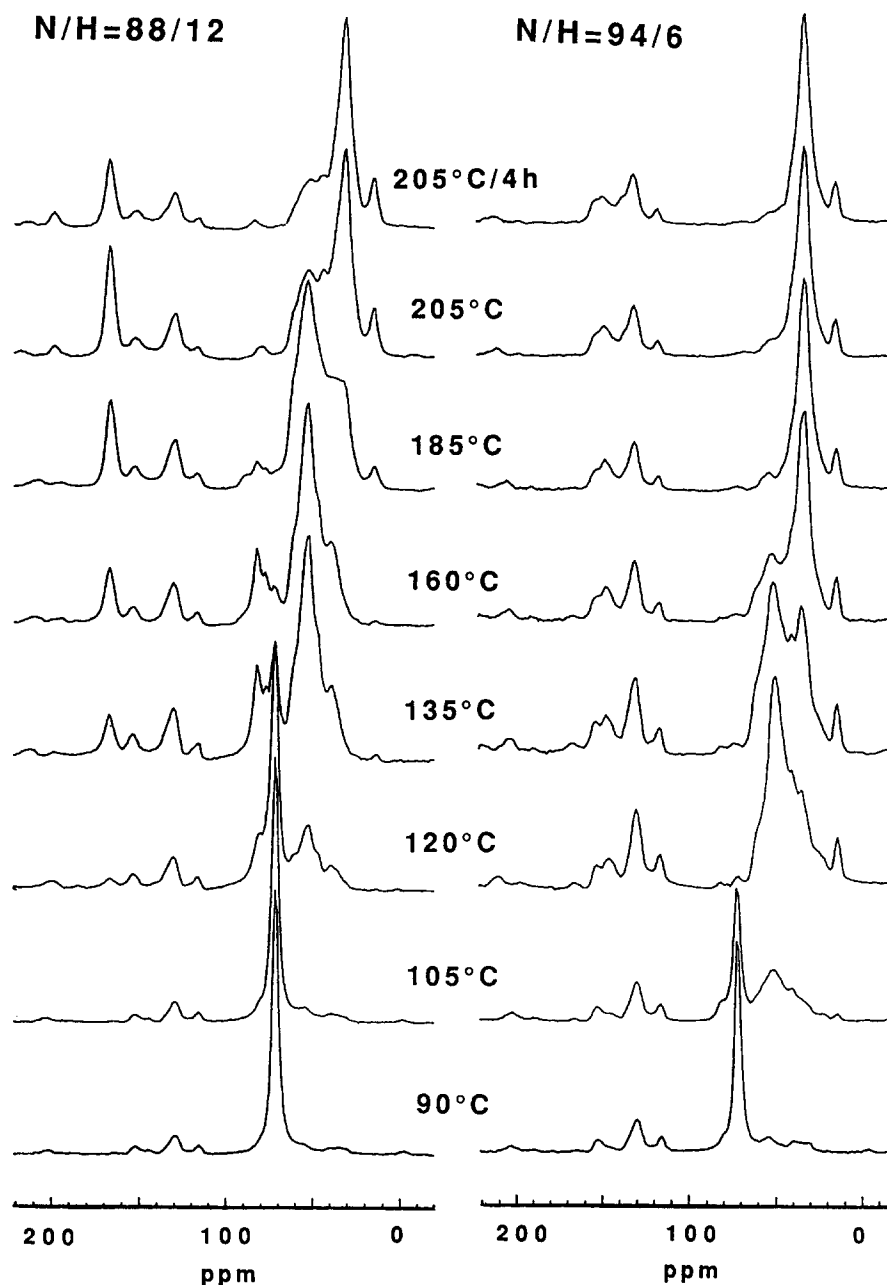


Figure 6  $^{13}\text{C}$  CP/MAS n.m.r. spectra of novolac/HMTA = 88/12 and 94/6 samples after curing (MAS rate = 4.2–4.6 kHz)

cured resins. But this resonance could not be detected in the 94/6 system after curing to 120°C (Figure 5). The minor peak around 85 ppm in the CP/MAS spectra (Figure 6) of this system is attributed to spinning side-bands since the rate of MAS in this case is 4.1–4.6 kHz. On the other hand, the resonances around 53 ppm (40–60 ppm, due to various substituted benzylamines) were significant at 120°C, and reached a maximum at 205°C for the 80/20 system, but at 185°C for the 88/12 system. For the 94/6 system, the resonance was very pronounced even at 105°C and decreased in intensity above 160°C (Figures 2 and 6).

(iii) *The lower the initial amount of HMTA in the system, the lower the temperature required to form methylene linkages.* Note that the intensity around 35 ppm (due to various *ortho-ortho*, *ortho-para* and *para-para* methylene linkages between phenolic rings) of the 80/20 system was weak after curing to 135°C, while that peak in the 94/6 system was very apparent at the

same temperature. On the other hand, the lower the initial HMTA content, the larger the number of methylene linkages formed. For the 80/20 samples after curing to 205°C/4 h (Figure 2), the peak at 35 ppm was not very strong, while the resonances around 53 ppm due to various curing intermediates were still pronounced. But the 35 ppm peak was dominant for the 94/6 sample cured to 205°C. The 88/12 system was intermediate between the two. Methyl groups at the *ortho* phenolic position (16 ppm) appeared simultaneously with the formation of the methylene bridges. Similarly, the lower the initial HMTA content, the lower the temperature at which these  $\text{CH}_3$  groups were formed.

(iv) *The lower the initial HMTA content, the lower the amount of the nitrogen-containing structures in the finally cured resins.* The resonance at 165 ppm has been assigned to the carbonyl carbons in amides/imides, and/or the  $-\text{CH}=\text{N}-$  carbon in imines. In the 80/20 system, it appeared at 135°C and remained in the final cured resins.



In the 94/6 system, this resonance was very weak, and disappeared above 160°C.

(v) *Decrease of the initial amount of HMTA brings about some different curing structures in the cross-linked network.* Both the solution (Figure 5) and the CP/MAS (Figure 6) n.m.r. spectra of the 94/6 system show resonances at 148–150 ppm, which were not observed in the other two systems. Furthermore, the intensities of these CH signals (detected by DEPT spectra) increased with curing temperature and remained in the fully cured sample. The strong intensity of the methine carbon resonance indicates that the carbons originate from HMTA, which is consistent with the formation of stilbenequinone structures (Table 1, (14)) as suggested previously<sup>26,27</sup>. The carbonyl carbons in the stilbenequinone rings (in the range 180–206 ppm) were too weak to be observed, because the resonances are not labelled.

#### <sup>15</sup>N CP/MAS n.m.r. spectra of cured novolac resins

The <sup>15</sup>N CP/MAS n.m.r. spectrum, with a wide chemical shift range for different structures, provides detailed information about structural changes during the curing process. During the initial stages of curing (below 120°C), no significant change could be observed in <sup>15</sup>N spectra for N/H = 80/20. The strong resonance at 41 ppm is due to the nitrogens in HMTA which are hydrogen bonded to the phenolic hydroxyl groups of the novolac<sup>10</sup>. The formation of various benzoxazine and

hydroxybenzylamine structures (as seen in <sup>13</sup>C spectra) just broaden the peak because their chemical shifts are similar to that of HMTA (Table 1). When the curing temperature was above 135°C, new resonances around 120 and 155 ppm appeared, and a resonance at 290 ppm appeared at 160°C, as shown in Figure 7. Their relative intensities increased with increasing curing temperature, and all of these resonances remained in the final cured resins up to 205°C/4 h. Meanwhile, the peak at 41 ppm shifts to 38 ppm as the curing temperature increases. For samples cured to 205°C, a narrow resonance was observed at 25 ppm. Similar to the 80/20 system, the <sup>15</sup>N spectra for the NH = 88/12 samples after curing to 105°C exhibited less change, and resonances at 120, 155 and 290 ppm were observed above 135°C, together with the shift of the peak at 41 ppm to 38 ppm at higher temperatures.

In Hatfield and Maciel's previous report<sup>10</sup>, the resonance at 290 ppm was not observed, and the peak around 120 ppm was assigned to spinning side-bands. We changed the spinning rate of MAS over the range 2–5 kHz for the N/H = 80/20 samples cured up to 185 and 205°C, but no spinning side-bands could be seen. All peaks observed in this report are real resonances. Considering the spinning rate (2.2 kHz) used in their work<sup>10</sup>, it is also difficult to assign the peak at 120 ppm to a spinning side-band of any resonance. The peaks at 38 ppm and 25 ppm were assigned to ammonium/benzylammonium ions, and

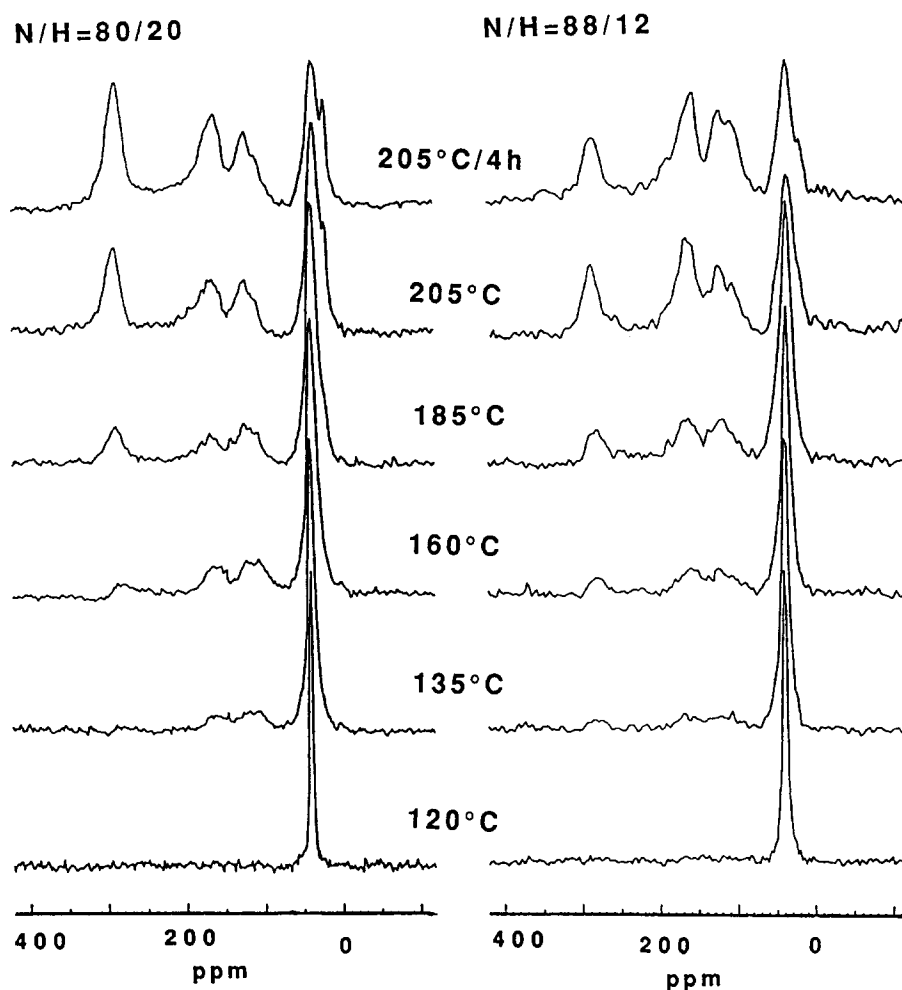
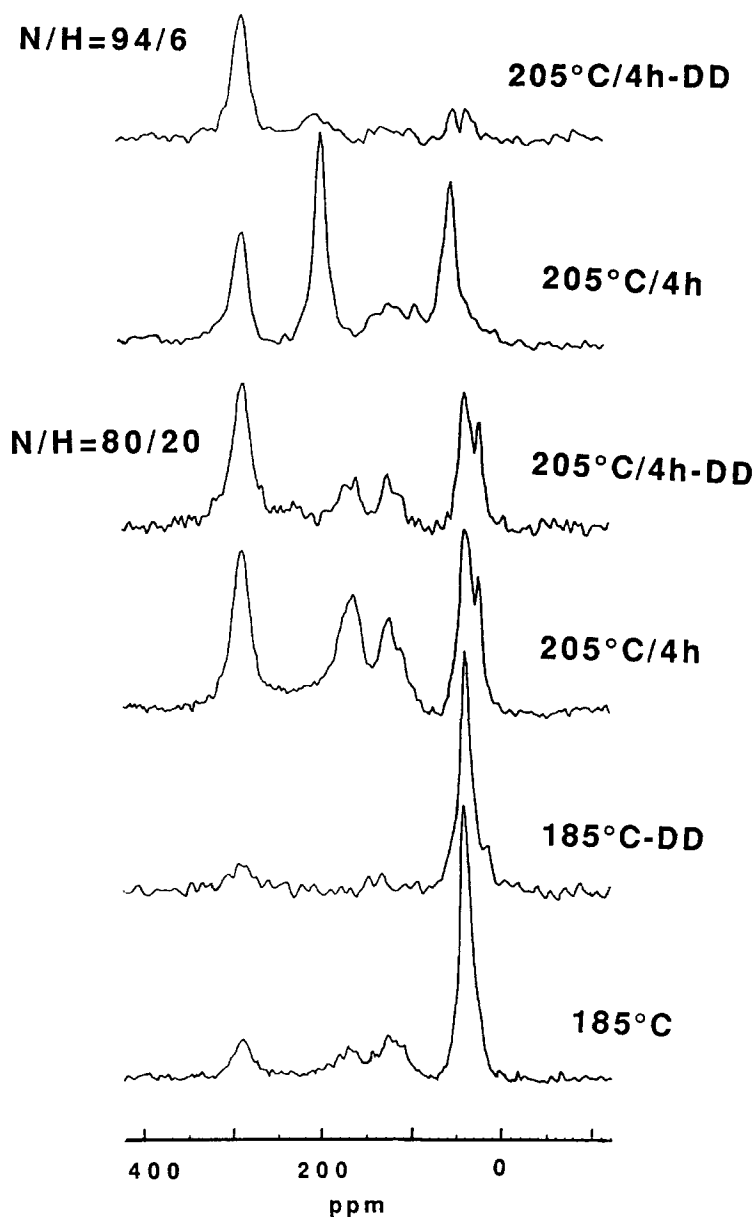


Figure 7 <sup>15</sup>N CP/MAS n.m.r. spectra of novolac/HMTA = 80/20 and 88/12 samples after curing



**Figure 8**  $^{15}\text{N}$  CP/MAS n.m.r. spectra and dipolar dephased spectra ( $130\ \mu\text{s}$  decoupling delay) of novolac/HMTA = 80/20 samples after curing to 185 and  $205^\circ\text{C}/4\text{h}$ , and the 94/6 sample after curing to  $205^\circ\text{C}/4\text{h}$

benzylamines, respectively<sup>10</sup>, while the peak at 290 ppm can be assigned to  $^{15}\text{N}$  in structures of imines<sup>22</sup>. These assignments are consistent with the results of dipolar dephased spectra shown in *Figure 8* for N/H = 80/20 samples. The nitrogen in most imines (except (13)-3) is not protonated, thus it should and did persist after a  $130\ \mu\text{s}$  decoupling delay. Meanwhile, the high mobility of ammonium/benzyl ammonium ions (38 ppm) and  $-\text{CH}_2\text{NH}_2$  groups (25 ppm) caused their  $^{15}\text{N}$  signals to remain in the dipolar dephased spectra. However, the resonances around 120 and 155 ppm had their intensities significantly decreased after a  $130\ \mu\text{s}$  decoupling delay, indicating that some of these nitrogens have protons attached. Hatfield and Maciel assigned the peak at 155 ppm to the nitrogen in an amide-type ( $\text{Ar}-\text{CH}_2-\text{NH}-\text{CHO}$ ) structure<sup>10</sup>. By comparison of chemical shifts for  $^{15}\text{N}$  in various amides and imides<sup>23</sup>, we assign the peak around 120 ppm to  $^{15}\text{N}$  in amide-type structures (*Table 1*, (11)), while that around 155 ppm is assigned to  $^{15}\text{N}$  in imide-type structures (*Table 1*, (12)). Since both resonances still persisted even after  $130\ \mu\text{s}$  decoupling

delay (*Figure 9*), structures with  $^{15}\text{N}$  resonances without attached hydrogens should be present as shown in *Table 1*, (11)-2, -3, -5 and -7 and (12)-2, -3 and -5.

The situation of the N/H = 94/6 system (*Figure 9*) is somewhat different from those of the 80/20 and 88/12 systems. A peak at 3 ppm due to trapped  $\text{NH}_3$  appeared in the spectrum of the sample cured to  $120^\circ\text{C}$ , and disappeared by evolution of ammonia as the curing temperature reached  $205^\circ\text{C}$ . This peak was not observed in the 80/20 and 88/12 systems. In addition, the imine structures (290 ppm) could be observed even at  $120^\circ\text{C}$ , a temperature that was significantly lower than those in the 80/20 and 88/12 systems. The amount of amide/imine-type structures in the cured N/H = 94/6 samples was also smaller. On the other hand, a resonance at 200 ppm initially appeared for the 94/6 samples cured up to  $160^\circ\text{C}$ , and then increased in intensity as the curing temperature increased. After the disappearance of resonances due to  $\text{NH}_3$  (3 ppm) and ammonium/benzyl ammonium ions (38 ppm), a new resonance at 58 ppm became dominant in the lower chemical shift range.

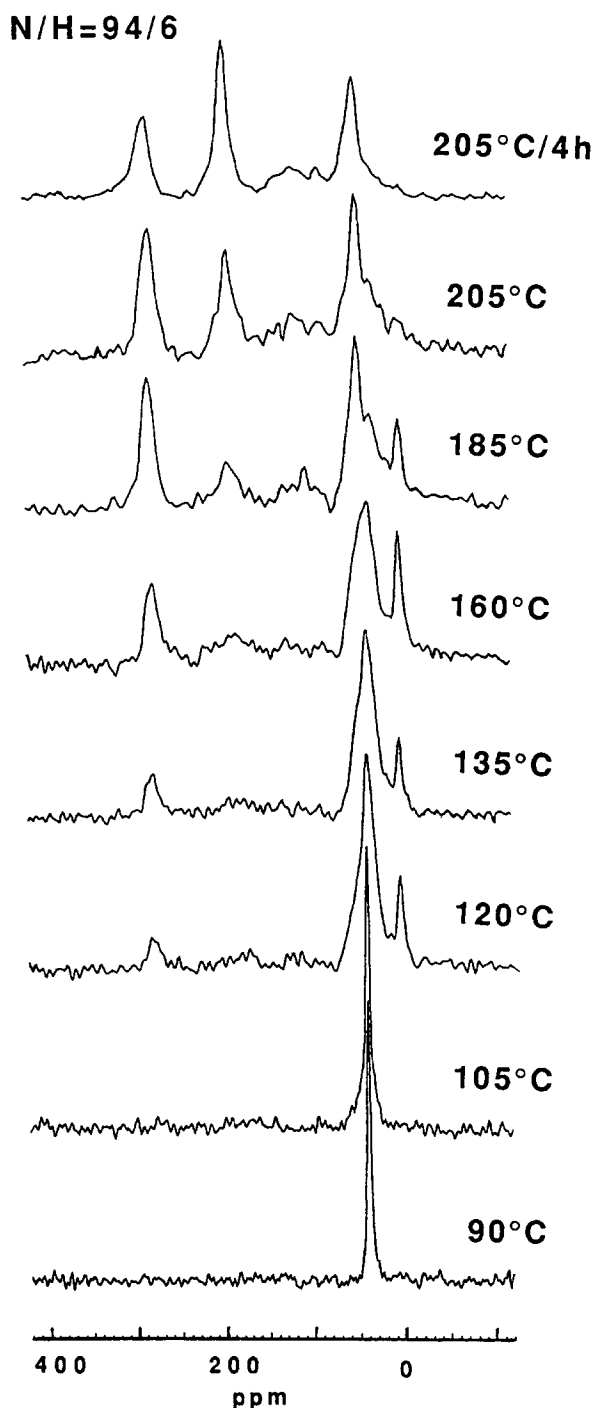


Figure 9  $^{15}\text{N}$  CP/MAS n.m.r. spectra of novolac/HMTA = 94/6 samples after curing

These two new resonances (at 200 and 58 ppm) correspond to protonated nitrogens in groups which are not mobile, because their intensities decrease dramatically in dipolar dephasing experiments (Figure 8). Here we summarize that the 200 ppm peak is due to an imine-type structure as shown in Table 1, (13)-3. In this structure the nitrogen is protonated, and the  $^{15}\text{N}$  signal should move to a lower chemical shift value than those of similar structures because the nitrogen has no bonded methylene or methyl group. The hydrogen attached to the nitrogen could hydrogen bond to other oxygen or nitrogen atoms in the system, causing an upfield shift of the signal. The 58 ppm peak may correspond to the nitrogen in structures such as shown

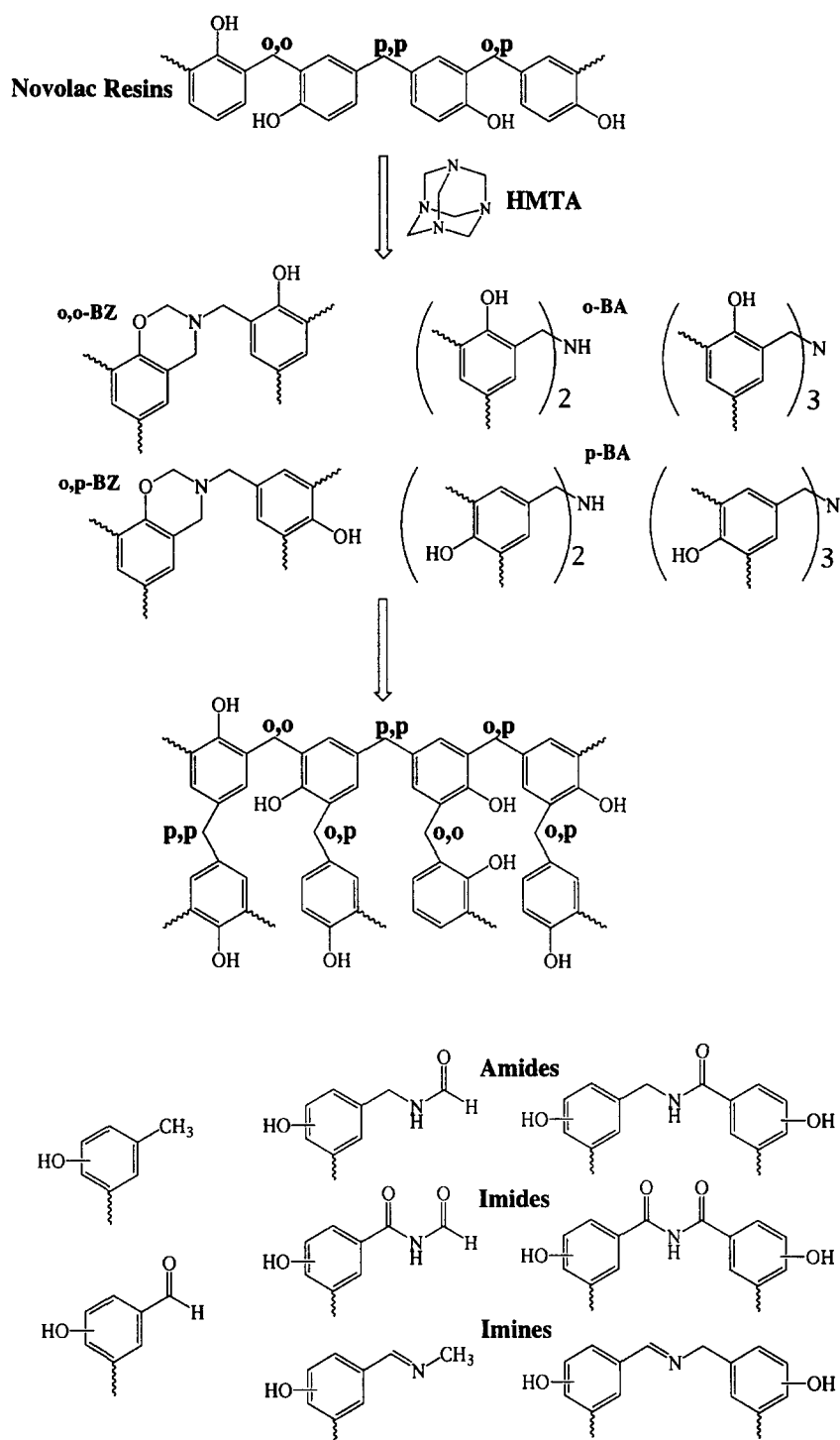
in Table 1, (13)-4, and -5, which originate from some reactions between intermediates and  $\text{NH}_3$  liberated during the curing. The results suggest that the chemical structures of the fully cured products and perhaps even the curing reaction pathways could be different if the initial amount of HMTA is varied, or the curing reaction pathways are the same but the temperatures at which the reactions occur are decreased when the HMTA content is low.

In summary, the above results indicate that the curing reaction consists of two stages as shown in Scheme 1: (i) the reactions between novolac resins and HMTA produce initial intermediates, mainly various substituted benzoxazines and benzylamines; (ii) the decomposition, oxidation and/or further reactions of these initial curing intermediates produce methylene linkages between phenolic rings, together with various amine, amide/imide, imine, and methyl phenol, benzaldehyde and other structures. During the curing process, many intermediates are formed, and some of these can even remain in the cured resins up to 205°C. Some intermediates reported here have not been reported previously while for others we provide evidence to establish pathways postulated in previous studies.

#### Curing chemistry of novolac resins

Several mechanisms for the initial stages of curing novolac by HMTA have been proposed. Early studies<sup>28,29</sup> suggested that the initial curing is a homogeneous acid-catalysed reaction involving a trace amount of water in the novolac to hydrolyse HMTA to  $\alpha$ -amino alcohols. The acidic phenolic units would generate carbonium ions from these  $\alpha$ -amino alcohols, which then react with phenolic units to form benzylamines. This postulate is supported by the fact that the reaction rate increases with decreasing pH for both the novolac resins and model systems<sup>15,30,31</sup> and increasing phenol<sup>31,32</sup> or water<sup>30,33-35</sup> content. Other claims suggested excess water could decrease the reaction rate<sup>36</sup>. An intermolecular hydrogen-bonding mechanism between novolac and HMTA was proposed by Katovic and Stefanic<sup>37</sup>. The nitrogens of HMTA can hydrogen bond to the phenolic protons in novolac chains that are originally self-associated through hydrogen bonding. As the temperature increases, two consecutive and temperature-dependent steps occur in the novolac reaction with HMTA: (i) the hydrogen of the phenolic hydroxyl transfers to HMTA nitrogen with the formation of ionized species; (ii) a hydrogen shifts from the *ortho* position of the ring to the oxygen anion. Then, the nucleophilic ring carbon anion attacks a methylene group of HMTA and forms an initial methylene bridge at the *ortho* position of the phenolic rings. Once the breakdown of the HMTA molecule has begun, further reactions occur via either protonation at the tertiary amine or all amines, and gives rise to derivatives of novolac. Our recent study<sup>38</sup> provided a definitive description of reactions between *ortho*- and *para*-phenolic sites of novolac resins and HMTA to produce benzoxazine and benzylamine intermediates by using xylenols as model systems.

A combination of  $^{13}\text{C}$  and  $^{15}\text{N}$  high-resolution solution and solid state n.m.r. studies allows the curing chemistry of novolac resins to be traced via the changes of the chemical structures throughout the curing process. Before curing, novolac and HMTA are hydrogen bonded



Scheme 1

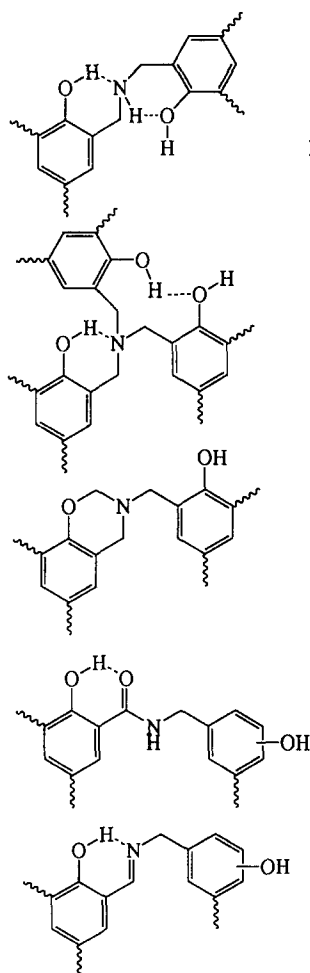
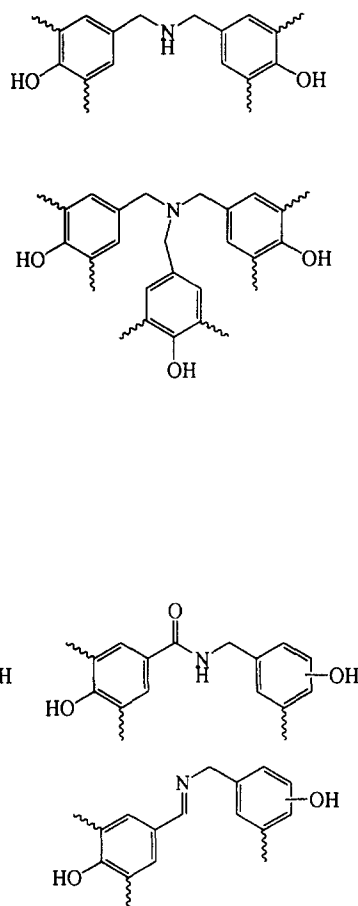
through the phenolic hydroxy group and the nitrogen of HMTA. This results in the phenolic C–OH carbon of N/H = 80/20, 88/12 and 94/6 systems shifting downfield by 1.5, 1.1 and 0.5 ppm, respectively. As the curing temperature initially increases to 90–120°C, the curing reactions start, and the initial intermediates formed are various substituted benzoxazine and benzylamine-type molecules. Triazine- and diamine-type structures and ether-type structures are also formed during the initial curing stage. This result is in agreement with previous reports, and the hydrogen-bonding mechanism discussed above<sup>37,38</sup>. Certainly, the curing reactions are very complicated, and a number of mechanisms may be involved. Further increasing the curing temperature

causes decomposition and further reactions of these initial intermediates to produce methylene linkages between phenolic rings for chain extension and cross-linking, together with amide-, imide- and imine-type intermediates by side-reactions such as oxidation and dehydrogenation, whereas NH<sub>3</sub> is liberated from the resins. Methyl-substituted products are also formed in the decomposition/reaction. A small amount of formaldehyde, liberated from the decomposition of the ether intermediates to produce methylene linkages, could also play a role in side-reactions. At high temperatures, various benzoxazine, benzylamine and imine intermediates could be oxidized by air to form various amide and imide structures. The aldehyde groups

and perhaps even carboxyl groups also occur in the oxidation. The  $^{13}\text{C}$  dipolar dephasing experiment and the  $^{15}\text{N}$  CP/MAS spectra show that imine structures and amide, imide structures with a  $>\text{N}-\text{CHO}$  group are formed at relatively lower temperatures. After the samples are cured to  $205^\circ\text{C}$ , amide and imide structures with  $\text{Ar}-\text{CO}-\text{N}<$  groups also occur, and some of these can remain in the fully cured resins. This result is consistent with the elemental analysis, which indicates 50–70% nitrogen loss and 20–30% oxygen gain after curing the N/H systems to  $205^\circ\text{C}/4\text{h}$ . The higher the initial amount of HMTA, the less nitrogen loss after curing to  $205^\circ\text{C}/4\text{h}$ . The contents of carbon and hydrogen decrease by about 5–7 and 5–10%, respectively, after fully curing. The benzylamine structures observed in fully cured samples could be side-products of the thermal decomposition. It does not necessarily mean that the initially formed benzylamines remain until  $205^\circ\text{C}/4\text{h}$ .

The initial HMTA content is critical to the curing rate and the chemical structure of the fully cured resins. The N/H weight ratios of 80/20, 88/12 and 94/6 correspond approximately to 1:1, 2:1 and 4.4:1 mole ratios of reactive sites in the novolac to methylenes in HMTA. Ideally, each methylene from HMTA would link two vacant reactive sites in the cross-linking if methylenes only act as the linkages. Among the various substituted benzylamines and their oxidation and decomposition

products such as amides, imides and imines, each reactive site links one  $-\text{CH}_2-$  originating from HMTA. In the benzoxazine structure, there are three  $-\text{CH}_2-$  from HMTA linked to two reactive sites. These intermediates can undergo thermal decomposition, while the free sites can also react with these initial intermediates or their decomposition products. With lower HMTA content such as that in the 94/6 system, the HMTA can provide only one  $-\text{CH}_2-$  linkage to 4.4 reactive sites of novolac. After the formation of the initial intermediates, many reactive sites remain and will react with those intermediates to produce further methylene linkages for cross-linking. This has been clearly evaluated in our current work on model systems, which will be published later. Therefore, the disappearance of most initial intermediates and the formation of a large number of methylene linkages occur at lower temperatures in the 94/6 system than in systems with higher HMTA ratios. In the latter, e.g. the N/H = 80/20 system, the HMTA can provide one  $-\text{CH}_2-$  linkage to each reactive site of novolac, and the formation of initial intermediates results in most reactive sites being used up. No additional reactive sites are available to react with these intermediates. As a result, many more nitrogen-containing intermediates are still present after curing to  $205^\circ\text{C}$  for the 80/20 system than for the 94/6 or 88/12 systems. On the other hand, the novolacs are acidic polymers while HMTA is a basic compound. The lower

*ortho*-Intermediates*para*-Intermediates

Scheme 2

the HMTA content, the lower the pH of the system, and the higher the reactivity of the system to form initial curing intermediates. A lower pH value is also beneficial to the decomposition and further reactions of the initial intermediates. Therefore, the lower the initial amount of HMTA, the higher the amount of methylene bridges formed at lower temperatures in the resins after curing. In addition, the curing pathways could also be somewhat different to produce a cross-linked network containing different side-products when the initial HMTA amount is low as seen in the 94/6 system.

We also note that the curing reactivity of *ortho*-reactive sites is different from those of *para*-reactive sites. In the  $^{13}\text{C}$  solution spectra (Figures 1, 4 and 5), the intensity of *para-para*  $-\text{CH}_2-$  resonances at 40.8 ppm always increases faster than those at 35.5 and 31.5 ppm (*ortho-para* and *ortho-ortho*  $-\text{CH}_2-$ ) as the curing temperature increases. This suggests that the *para*-linked intermediates are less stable and more easily decompose or undergo further reactions to form the methylene linkages. The stability of the *ortho*-linked intermediates can be attributed to structural reasons and the intramolecular hydrogen-bonding interaction. As seen in Scheme 2, benzoxazine has a stable six-membered ring structure, and other *ortho*-linked intermediates such as (*ortho*-hydroxybenzyl)amines, *ortho*-linked amide, imide and imine structures can all form intramolecular hydrogen bonds with a six-membered ring structure, which can stabilize the intermediates. This is not possible for *para*-linked intermediates, where only intermolecular hydrogen bonding is possible. Therefore, *para*-linked curing intermediates are less stable and decompose and/or undergo further reactions at relatively lower temperatures. This has been confirmed in our curing study of various model oligomers, which will be published shortly.

In conclusion, this investigation on the curing of novolac resins with HMTA provides a comprehensive understanding of the curing chemistry, and indicates that the chemical structures of the final cured novolac resins can be controlled by variation of the initial amount of HMTA and the ratio of *para*-/*ortho*-reactive sites of the original resins. In order to obtain a cross-linked novolac network with more stable nitrogen-containing structures, a relatively large amount of HMTA and resins with more *ortho*-reactive sites should be used. By contrast, using a small amount of HMTA and resins containing a high number of *para* sites generates a low nitrogen-containing cross-linked network. If the initial amount of HMTA is very small, the curing pathways can be different, and result in a cross-linked network containing different kinds of side-products. The  $^{13}\text{C}$  and  $^{15}\text{N}$  n.m.r. spectra of the resins observed at the increased curing time also reflect the dynamics of the curing reaction and the abundance of the intermediate species. The details will be discussed in our study of model novolac systems which are less complicated, and can thus provide more distinct information on the kinetics of the curing reactions

#### ACKNOWLEDGEMENTS

This work was supported by the Australian Industry Research and Development Board (Grant No. 15068), the Australian Research Council, and Comalco

Aluminium Ltd. We thank Mr M. J. Caulfield for preparing the  $^{13}\text{C}$ - and  $^{15}\text{N}$ -labelled HMTA, and Mr A. C. Potter for discussions.

#### REFERENCES

- Martin, R. W., *Chemistry of Phenolic Resins*. Wiley, New York, 1956.
- Megson, N. J. L., *Phenolic Resin Chemistry*. Butterworths, London, 1958.
- Knop, A. and Scheib, W., *Chemistry and Application of Phenolic Resins*. Springer-Verlag, New York, 1979.
- Knop, A. and Pilato, L. A., *Phenolic Resins*. Springer-Verlag, New York, 1985.
- Fyfe, C. A., Rudin, A. and Tchir, W. J., *Macromolecules*, 1980, **13**, 1320.
- Fyfe, C. A., McKinnon, M. S., Rudin, A. and Tchir, W. J., *Macromolecules*, 1983, **16**, 1216.
- Bryson, R. L., Hatfield, G. R., Early, T. A., Palmer, A. R. and Maciel, G. E., *Macromolecules*, 1983, **16**, 1669.
- Maciel, G. E., Chuang, I.-S. and Gollob, L., *Macromolecules*, 1984, **17**, 1081.
- So, S. and Rudin, A., *J. Polym. Sci., Polym. Lett.*, 1985, **23**, 403.
- Hatfield, G. R. and Maciel, G. E., *Macromolecules*, 1987, **20**, 608.
- Amram, B. and Laval, F., *J. Appl. Polym. Sci.*, 1989, **37**, 1.
- Sinha, H. R. and Blum, F. D., *J. Appl. Polym. Sci.*, 1989, **37**, 163.
- Chuang, I.-S. and Maciel, G. E., *Macromolecules*, 1991, **24**, 1025.
- Pethrick, R. A. and Thomson, B., *Br. Polym. J.*, 1986, **18**, 380.
- Kopf, P. W. and Wagner, E. R., *J. Polym. Sci., Polym. Chem.*, 1973, **11**, 939.
- Sojka, S. A., Wolfe, R. A., Dietz, Jr. E. A. and Dannels, B. F., *Macromolecules*, 1979, **12**, 767.
- Sojka, S. A., Wolfe, R. A. and Guenther, G. D., *Macromolecules*, 1981, **14**, 1539.
- Bogan, Jr. L. E. *Macromolecules*, 1991, **24**, 4807.
- Bogan, Jr. L. E. and Wolk, S. K., *Macromolecules*, 1992, **25**, 161.
- Dargaville, T., de Bruyn, P. J., Lim, A. S. C., Looney, M. G., Potter, A. C., Solomon, D. H. and Zhang, X., *J. Polym. Sci., Polym. Chem.*, in press.
- Potter, A. C., Ph.D. thesis, University of Melbourne, 1996.
- Levy, G. C. and Lichter, R. L., *Nitrogen-15 Nuclear Magnetic Resonance Spectroscopy*. Wiley, New York, 1979.
- Sadtler Research Laboratories, *The Sadtler Standard Carbon-13 n.m.r. Spectra*. Philadelphia, 1977.
- Levy, G. C., Lichter, R. L. and Nelson, G. L., *Carbon-13 Nuclear Magnetic Resonance Spectroscopy*. Wiley, New York, 1980.
- Mihajlovic, M. L. and Cekovic, Z., in *The Chemistry of the Hydroxyl Group*, ed. S. Patai. Interscience, New York, pp. 505-592.
- Zinke, A., *J. Appl. Chem.*, 1951, I, June, 257.
- Cook, C. D., Nash, N. G. and Flanagan, H. R., *J. Am. Chem. Soc.*, 1955, **77**, 1783.
- Hultzsch, K., *Ber. Dtsch Chem. Ges.*, 1949, **82**, 62.
- Duff, J. C. and Furness, V. I., *J. Chem. Soc.*, 1951, 1512.
- Kamenskii, I. V., Kuznetsov, J. N. and Moiseenko, A. P., *Vysokomol. Soedin. Ser. A*, 1976, **18**, 1787.
- Keutgen, W. A., *Encyclopedia of Polymer Science and Technology*, Vol. 10. Interscience, New York, 1969, pp. 1-73.
- Takamitsu, N., Okamura, T. and Nishimura, M., *Nipp. Kag. Kaishi*, 1973, 2196.
- Tonogai, S., Sakaguchi, Y. and Seto, S., *J. Appl. Polym. Sci.*, 1978, **22**, 3225.
- Tonogai, S., Hasegawa, K. and Kondo, H., *Polym. Eng. Sci.*, 1980, **20**, 1132.
- Basov, N. I., Kazankov, Y. V., Leonov, A. I., Lynbartovich, V. A. and Mironov, V. A., *Izv. Vyssh. Ucheb. Zaved., Khim. Khim. Tekhnol.*, 1969, **12**, 1578.
- Wang, X., Riedl, B., Christiansen, A. W. and Geimer, R. L., *Polymer*, 1994, **26**, 5685.
- Katovic, Z. and Stefanic, M., *Ind. Eng. Chem. Prod. Res. Dev.*, 1985, **24**, 179.
- Looney, M. G. and Solomon, D. H., *Aust. J. Chem.*, 1995, **48**, 323.